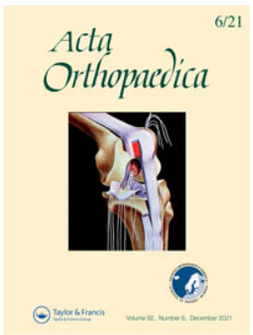

Acta Orthopaedica Scandinavica

ISSN: 0001-6470 (Print) (Online) Journal homepage: informahealthcare.com/journals/iort19

Rapid bone and blood flow formation in impacted morselized allograftsPositron emission tomography (PET) studies on allografts in 5 femoral component revisions of total hip arthroplasty

Jens Sörensen, Gösta Ullmark, Bengt Långström & Olle Nilsson

To cite this article: Jens Sörensen, Gösta Ullmark, Bengt Långström & Olle Nilsson (2003) Rapid bone and blood flow formation in impacted morselized allograftsPositron emission tomography (PET) studies on allografts in 5 femoral component revisions of total hip arthroplasty , Acta Orthopaedica Scandinavica, 74:6, 633-643, DOI: 10.1080/00016470310018126

To link to this article: https://doi.org/10.1080/00016470310018126

Published online: 08 Jul 2009.

Acta Orthopaedica Scandinavica Award article 2003

Rapid bone and blood flow formation in impacted morselized allografts

Positron emission tomography (PET) studies on allografts in 5 femoral component revisions of total hip arthroplasty

Jens Sörensen[2], Gösta Ullmark[1], Bengt Långström[2] and Olle Nilsson[3]

[1]Department of Orthopedics, Länssjukhuset, Gävle, [2]PET-center Uppsala University, Uppsala, [3]Department of Orthopaedics Uppsala University Hospital, Uppsala, Sweden
Correspondence: gosta.ullmark@lg.se
Submitted 02-09-16. Accepted 03-05-07

ABSTRACT 5 patients were revised with impaction of morselized frozen allograft and a cemented total hip arthroplasty (THA) because of loosening and osteolysis of a primary hip arthroplasty. Plain film radiographs of the stems showed stable implants in all patients 15–24 months after surgery. The clinical results were good. We used: 1) Positron Emission Tomography (PET) to evaluate vascularization and new bone formation in the allograft, 2) kinetic [^{18}F]-fluoride PET to produce quantitative images, interpreted as new bone formation in the allograft surrounding the femur stem, 3) [^{15}O]-water PET to quantify bone blood flow, and 4) [^{15}O]-carbon monoxide to determine blood volume. After surgery, all patients were evaluated twice: at 1–8 days and 12 months and 3 patients were also studied at 4 months. As early as at 8 days after surgery, blood flow and bone formation had increased greatly adjacent to the allograft. At 4 months blood flow and bone formation were about the same, but activity was highest in the graft material. At 1 year after surgery, blood flow had declined to the levels of the contralateral femur diaphysis in most of the graft bed. These findings using the PET technique showed that angiogenesis and new bone formation occurred early after impaction of morselized bone allografts around the femoral component in revision THA. We found that PET is a sensitive method for evaluating neovascularization and bone formation in the graft beds.

The use of impacted morselized bone allograft in revision total hip arthroplasty for prosthetic loosening has gained widespread acceptance during the last decade. However, the results have varied considerably. Subsidence of the femoral stem occurs in 0–86% of the patients (Kärrholm et al. 1999, Mikhail et al. 1999, Nivbrant et al. 1999), and the failure rates in terms of mechanical loosening vary from 0–4% after 5 years (Nivbrant and Kärrholm 1999, Ullmark et al. 2002), to 10% already after 1 year (Eldridge et al. 1997) and 19% after 5 years (van Biezen et al. 2000).

Despite the widespread clinical use of impaction bone allografts, little is known about the physiological events that take place in the graft bed during the first year. The histological findings in biopsies from 4 patients the second year after impaction have been reported (Nelissen et al. 1995). Morphological studies of graft material from biopsies and autopsies of 14 patients, of which 5 were done in the first year after surgery, have also been described (Linder 2000). The findings in biopsies of the proximal femur in 18 patients examined 1–11 months after surgery (Ullmark and Obrant 2002), and one retrieval proximal femur 6 months after surgery have also been reported (Ullmark and Linder 1998). These clinical studies show a slow in- and on-growth of new bone onto the surfaces of the allograft granules, with a very slow rate of graft

Table 1. Details of the 5 patients

Case	Gender	Age at revision	Removed implant [a]	Bone loss [b]
1	F	54	4	III
2	M	65	3	IV
3	F	75	1	II
4	M	77	2	III
5	F	73	1	II

[a] Type of implant removed
1 Lubinus SP
2 Charnley
3 PCA
4 unknown cementless stem implanted in Poland
[b] Endo Klinik Classification II–IV

resorption. Soft tissue ingrowth seems to precede bone formation.

To understand better the biological response of morselized bone allografts we studied the dynamics of bone blood flow and the rate of mineralization with Positron Emission Tomography (PET) during the first year after surgery in 5 patients who underwent revision THA.

PET is a nuclear medicine method for studying metabolic events. It has been established as a valuable research tool in many areas of life science. Various substances are labeled with radioactive isotopes. These labeled compounds are given in tracer amounts and detected by the scanner using a tomographic approach. The resulting 3-dimensional images represent the concentration of the labeled substance in the tissue, reflecting a metabolic event. Up till now, however, PET has hardly been used in orthopedics. A comparison of PET and gamma camera-based techniques in orthopedic research showed that PET may be better for several reasons, recently summarized by Blake et al. (2001).

Patients and methods

Patients

5 patients (3 women) with ages ranging from 54 to 77 years were included in the study (Table 1). All had been treated with a revision THA and impaction bone allografting due to mechanical loosening of a primary THA together with a loss of bone, grades II–IV, according to the Endo Klinik Classification (Engelbrecht and Heinert 1987). The primary THA had been performed because of osteoarthrosis in 4 patients and fracture sequelae in 1. The revision THAs had been done in 1998 or 1999 by one surgeon (GU) well acquainted with the surgical technique (described below). The contralateral hip was healthy and had not been subjected to previous surgery in 4 patients, while 1 had had a functional THA. In 4 of the patients the acetabular component was also revised, in 3 of the 4 with impaction grafting.

The study was approved of by the Ethics Committee, Uppsala University (no. 98454).

Surgical technique

Dedicated impaction instruments were used together with a cemented, matte and collared Lubinus SP II stem (Waldemar Link GmbH & Co, Hamburg, Germany). The size of the phantom was selected to permit a theoretical 2–3.5 mm thick cement mantle around the stem.

All patients were given systemic antibiotic prophylaxis during surgery. The operation was performed via a posterior surgical approach. The loose prosthesis, cement, debris and fibrous membrane were removed and the sclerotic inner surface of the bone was roughened with a cutter, then thoroughly irrigated.

The femoral cavity was occluded by a sturdy fitting acrylic plug (Mitab, Scandimed, Sjöbo, Sweden) inserted with a centralizing rod and placed at least 1 cm distal to the most distal osteolysis. The entire cavity was filled with corticocancellous allograft using distal impactors. The appropriate double-tapered phantom chosen for the femoral component was then driven on the centralizer down into the grafted cavern producing a firm graft impaction. Finally, the proximal centimeters between the femoral cortex and the phantom were impacted with a proximal impactor.

Using a small catheter connected to a suction device, all liquid was removed from the central canal inside the phantom. Antibiotic-loaded cement (Palacos with Gentamicin, Scheering-Plough Kenilworth NJ) was introduced with a narrow nozzled cement gun to fill the cavity in a retrograde direction. The phantom was removed just before to the insertion of the cold bone cement. The femoral

Table 2. Tracers used in postoperative PET analyses of the 5 patients

Case	1 day	8 days	4 months	12 months
1	–	^{18}F, ^{15}O	^{18}F, ^{15}O	^{18}F, ^{15}O
2	–	^{18}F, ^{15}O	^{18}F, ^{15}O	^{18}F, ^{15}O
3	–	^{18}F, ^{15}O	^{18}F, ^{15}O	^{18}F, ^{15}O
4	–	^{18}F, ^{15}O	–	^{18}F, $C^{15}O$
5	^{18}F, $C^{15}O$, ^{15}O	–	–	^{18}F, ^{15}O

^{18}F, radioactive fluorine, reflects bone healing.
^{15}O, radioactive water, measures blood flow.
$C^{15}O$, radioactive carbon monoxide, assesses blood volume.

component was inserted while the cement still had a low viscosity. After the cement had cured, we selected an appropriate neck length.

Bone grafting

Bone grafts, from fresh frozen femoral heads harvested at primary arthroplasty for hip osteoarthrosis, were stored at minus 80 °C. Before morselizing, most of the cartilage and fibrous tissue were removed from the femoral heads. The bone was morselized with a Howex milling machine (Gävle, Sweden). This machine produces chips of sizes up to a maximum of 2 × 4 × 5 mm (measured after impaction) (Ullmark 2000). The milled bone chips were partly defatted by rinsing in warm saline solution (40 °C).

Postoperative care

All patients were treated with low molecular weight heparin for thrombosis prophylaxis for 9–21 days. They were mobilized on the first to the third day after surgery by being allowed to walk with toe-touch weight-bearing on the operated leg, using two crutches for the next 3 months. Antibiotics were given systemically for 3 days. On the first day cefuroxime was given in a dose of 1.5 g × 3 and on the following 2 days, flucloxacillin was given in a dose of 1.5 g × 2. None of the patients had NSAID drugs postoperatively.

PET analyses

Scanners

We used two PET scanners, a GE Scanditronix 4096 scanner (GE Scanditronix, Uppsala, Sweden 1990) for the first 3 patients and a Siemens/CTI Exact HR + scanner (Siemens/CTI, Knoxville, TN 1999) for the last 2. The GE 4096 has a field of view (FOV) of 10 cm and yields 15 consecutive transaxial slices. The HR+ has a FOV of 15 cm, yielding 63 transaxial slices. The scanners were cross calibrated.

Patient preparatŠn

Patients were placed in the supine position on the camera bed. A vacuum cushion fixated the legs. A 25-gauge arterial catheter was inserted into the radial artery for blood sampling. A venous catheter was inserted into an antecubital or dorsal hand vein for injection of tracers. When [^{15}O]-carbon monoxide was used, we inserted a nasal catheter for inhalation of the radioactive gas. The catheter tip was then carefully positioned in the nasopharynx at the level of the soft palate. Table 2 shows the measurements that we made during the study.

TransmissŠn scans

Because the FOV of a standard PET scanner is limited to 10–15 cm, the part of the femoral stem in the gantry must be carefully positioned. This was done by short repetitive 2 min. transmission scans, which were rapidly reconstructed to form graphical volumetric density maps, on which metal implants are easily located. The bed was then moved to let the FOV encompass the distal part of the prosthesis. After positioning, a 10 min. transmission scan was taken to produce a more correct density map used for subsequent attenuation correction. In the cases where the scanner with the smaller FOV was used, an additional 10 min transmission scan was performed 10 cm. proximal to the first one.

[^{15}O] H_2O scans

15–20 MBq/kg of water labeled with ^{15}O was injected into an antecubital vein as a rapid bolus. At the same time we started a camera protocol with time frames of 23 × 5 s, 2 × 20 s and a vacuum pump connected to the arterial line for continuous blood sampling. Blood was withdrawn at a rate of 3 mL/min through a scintillation counter, cross calibrated to the camera, and with a report rate of 1/sec. Measurements in blood were decay-corrected to the start of the scan.

[^{15}O] CO scans

^{15}O-labeled carbon monoxide was delivered directly from the cyclotron to a mixing chamber (GE PETgas 2000, GE/PETT Electronics Inc, St. Louis, MO). Labeled gas mixed with air was continuously inhaled for 120 seconds at a flow rate of 1.5 L/min through a nasal catheter. After gas delivery was stopped, 60 s was allowed for equilibration of CO in the blood. The scanner was then started with a protocol of 5 × 60s time frames. Radioactivity in blood was measured by discrete samplings at 1, 2.5 and 4 min after and decay-corrected to the start of the scan. The last blood sample was checked for hemoglobin-CO for patient safety.

[^{18}F] fluorine scans

When ^{15}O-tracers had decayed to background levels and no distorting radioactivity remained in the tissue, 180–380 MBq of [^{18}F] fluorine in 5 mL saline was injected intravenously as a bolus with a subsequent saline flush. The scanner was started at the same time as the injection with a protocol of 5 × 60 s, 5 × 180 s and 6 × 300 s time frames. Arterial blood samples were taken at 0.5, 1, 2, 3, 5, 7, 10, 15, 20, 25, 30, 40 and 50 min after injection. In one patient, arterialized venous blood from a dorsal hand vein preheated to 42 °C was used, because of difficulties in maintaining a patent arterial line. After centrifugation, the concentration of radioactivity in plasma was measured and decay-corrected to the start of the scan. When using the scanner with a 10-cm FOV, only a small part of the graft bed was studied dynamically. In these cases, we moved the bed 10 cm and obtained a single time frame of 10 min. to visualize more of the femoral stem area.

Image processing

All emission scans were corrected for attenuation, scatter and decay and reconstructed by a process of filtered-back projection. We used a 4.2 mm Hann filter to obtain an image resolution of 7 and 6 mm in-plane FWHM for the two scanner types.

The dynamic information from the ^{18}F studies was converted to pixel-based images of fluoride net clearance (K_{PAT}) by the Gjedde-Patlak graphical analysis (Gjedde 1981, 1982. Patlak et al. 1983). This calculation is a simplification of a 3-compartment model, based on the assumption that the tracer is irreversibly trapped intracellularly during the study. This means that the rate at which fluoride ions are cleared from plasma and incorporated into bone mineral can be calculated and presented in color-coded images. The clearance is defined as the slope of the linear relation of the tracer distribution volume (tissue concentration as measured by the scanner at time T divided by plasma concentration) as a function of the plasma integral divided by plasma concentration at time T. The slope was estimated by least squares fitting, omitting the initial 20 minutes. In the absence of positron emitting isotopes of calcium and phosphorus, ^{18}F-fluoride is used and a close relation between K_{PAT} and the true clearance of calcium is assumed. Likewise, for the K_{PAT} to be meaningful in serial studies, the intra- and extracellular pools of native calcium, phosphate and fluoride ions are assumed to be relatively equal over time and between subjects. The Gjedde-Patlak plot has been compared and validated using ^{18}F against a full 3-compartmental model by several investigators (Hawkins et al. 1992, Piert et al. 1998). We also calculated Standardized Uptake Values (SUVs) from summed activity images 35–50 min after injection and from the static images obtained from secondary locations of the stem area. SUV was calculated by the formula: SUV of tissue = activity in tissue (Bq/mL) * body weight (gram)/total injected dose (Bq). By setting the average body density at 1 g/mL, this expression gives a unitless value of the regional tissue activity in proportion to the average activity per mL of the entire body.

Bone blood flow was assessed from the [^{15}O] water scans by using an autoradiographic method (Raichle et al. 1983). We set the tissue distribution volume of water at 0.95, which is an average in soft tissue. We chose this value, because the graft bed supposedly undergoes changes from non-viable through highly vascularized granulation tissue and finally mineralization. So far as we know, the true distribution volume of water is not known in any of these situations. The model also requires that the tracer of choice diffuse freely in the tissue. We assumed that water fulfilled this criterion in bone. Finally, the model deconvolves the stimulus response function—i.e., the tissue time-activity curve—by the input function—i.e., the arterial time-activity curve. Because the blood curve is

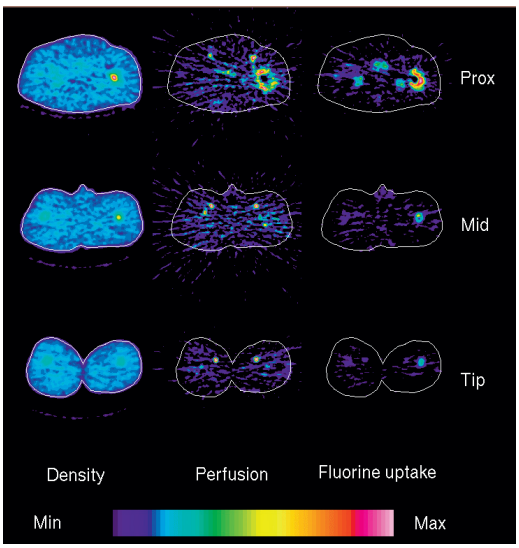

Figure 1. Density, blood flow ([^{15}O]-water), and bone formation ([^{18}F]-fluoride) PET in patient number 2 at 4 months.

measured by sampling from a catheter in the radial artery, the shape of this curve will differ from that of the true femoral artery. To account for this difference in shape, the blood curve measured was corrected for curve dispersion and delay. These parameters were estimated by an extension to the model program by use of the count rates file produced by the scanner and an iterative least squares fitting routine. The integration time was fixed at 180 seconds. Similar methods have been used to study bone blood flow quantitatively and been found to give reliable results (Ashcroft et al. 1992, Piert et al. 1998).

According to our literature search, absolute quantification of bone blood volume using [^{15}O] CO has only been tried once (Iida et al. 1999). The application and calculations of this technique are relatively straightforward. Labeled carbon monoxide is inhaled and is irreversibly trapped in erythrocytes. When labeled cells are mixed uniformly in the blood pool, the concentrations of radioactivity measured regionally by PET in relation to whole blood samples measured externally is proportional to the regional blood volume. The hematocrit in capillaries differs from that in whole blood. Since a variable portion of the blood pool is contained in the capillaries, tissue blood volume must be corrected. We used a factor of 0.85.

Image analysis

Regions of interest (ROI) were defined graphically on attenuation maps derived from the transmission scans and exported to SUV and Patlak images of [^{18}F]-fluoride as well as images of blood flow and blood volume (Figure 1). Circular ROIs with a diameter of 25–30 mm were placed on several transaxial slices over femoral diaphysis contralateral to the graft bed and used as a reference region. A single circular ROI with a radius of 10 mm was placed 1 cm distal to the prosthesis tip, corresponding to Gruen zone IV (Gruen et al. 1979). Circular ROIs were also placed on transaxial slices of the graft bed with a diameter equal to the diameter of the prosthesis plus 4 mm to account for the cement layer. The circular ROIs surrounding the prosthesis were expanded to form 6 mm wide doughnut-like rings, thus covering inner parts of cortical bone of the diaphysis and most of the graft layer, but leaving out cement and metal stem. Mean ROI values from each type of image were obtained for further analysis.

The values of all measurements are presented for anatomical locations corresponding to Gruen zones. TIP corresponds to zone IV; MID corresponds to zones III and V (i.e., 5 cm above the tip of the stem). More proximal areas are presented when applicable. Average values of the contralateral healthy femur are also presented, denoted as REF in the text. Because of the limited axial field of view of the PET, MID was chosen as a primary focus of interest and was analyzed in all studies, while other locations were not available in all patients.

Profiles from at least 4 different angles through the center of the femoral shaft 5 cm proximal to the prosthesis tip were also analyzed. The profiles (Figure 3) show activity levels along the line drawn. The peak-to-peak distance was recorded for each angle and averaged.

RadŠgraphical and clinical examinatŠns

Plain radiographs, anterior and lateral views, were taken post-operatively and at follow-up (15–24 months after surgery). The radiographs were analyzed in consensus by one of the authors (GU) and a radiologist. Clinical examination was performed preoperatively and at follow-up. The Charnley modification of Merle d'Aubigné-Postel classification was used (Charnley 1979).

Table 3. Clinical and radiographic findings

Case	Healing of trochanter osteotomy	Radiographic findings [a]	Clinical results [b] preop./postop.
1	+	1:IV 2:I–VII	10/18
2	–	1:VII 2:VII	9/16
3	+		14/17
4	+		12/18
5	+	2:V	13/18

[a] Radiographic findings: 1: Cortical healing, 2: New trabecular formation in Gruen zones I–VII .
[b] Merle d'Aubigné-Postel Score 1–18

Statistics

Numerical results are presented as mean (SD), unless otherwise stated. Differences in mean values were assessed with non-parametric Wilcoxon matched pairs test. Correlation of kinetic and static [^{18}F] fluorine uptake in bone was calculated with simple linear regression analysis. A p-value of < 0.05 was considered significant.

Results

Clinical and radŠgraphical results

The clinical outcomes were good in all patients (Table 3). 2 patients had a slight residual pain, one because of non-union of a trochanteric osteotomy (mentioned above), the other because of a tendinitis.

No subsidence was seen for any of the femoral stems on plain radiographs. The granular appearance of the graft bed visible on post-operative radiographs had disappeared after 1 year in all cases. New trabecular bone formation was most prominent in Gruen zone VII, which correlates to the area where the bone graft is most loaded. Cortical healing and new trabecular formation are presented in Table 3 for the patients evaluated after 2 years.

PET results

Mean values of quantitative ^{18}F uptake and bone blood flow in various regions over time are presented in Figure 2.

Day 1 after surgery (patient 5 only) the femoral shafts were clearly visualized bilaterally on 18F images. SUVs in the grafted areas were homogeneous and in level with the contralateral side. Absolute values of K_{PAT} and blood flow were not available because of arterial blood sampling errors. However, no elevation of relative blood flows was seen, comparing grafted to non-grafted femurs. In contrast, relative muscle blood flow was increased by 80% on the grafted side compared to non-grafted side. Average blood volume was 2.7 and 3.5 mL/100mL in grafted and non-grafted femur, respectively.

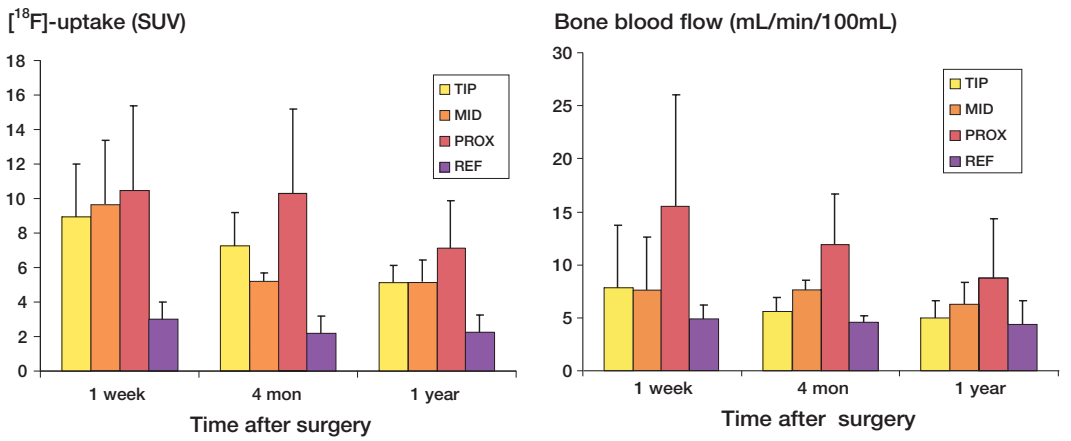

Figure 2. Mean values of [^{18}F]-fluoride uptake (left) and bone blood flow (right) over time. Measurements were made 1 cm distal to the prosthesis tip (TIP), 5 cm proximal to the tip (MID), 10–15 cm proximal to the tip (PROX) and in the healthy contralateral diaphysis of the femur (REF). The number of samples varies from 3 to 6.

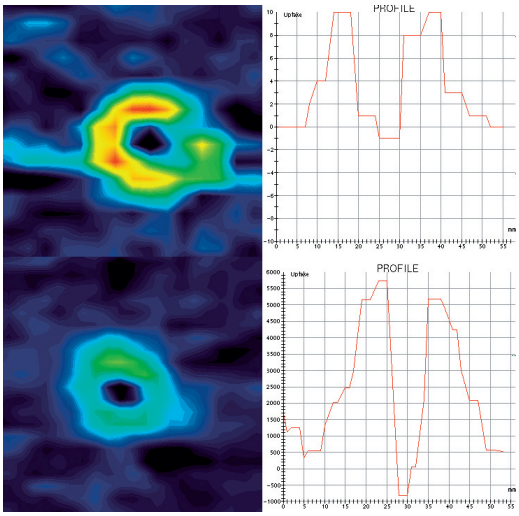

Figure 3. Peak-to-peak distance of transverse sections using ^{18}F PET in patient number 2 at 1 week and 1 year.

8 days after surgery (patients 1–4), large regional variations were seen with prominent elevation of blood flow around the proximal graft bed both in bone tissue and in muscle tissue, but close to normal levels (relative to contralateral structures) more distally in all patients. Mean blood flow in the grafted bone area averaged 8.7 mL/min/100 mL and in REF 4.9 mL/min/100 mL). In patient 2 an extreme increase in blood flow was seen in a posterior bone region proximally, reaching up to 35 mL/min/100 mL. This region corresponded to a known cortical defect of 5 × 3.5 cm, where a titanium mesh and cerclage wires covered a thick graft bed.

Fluorine uptake showed a definite gradient with higher average uptakes proximally. K_{PAT} (min^{-1}) was 0.043 (0.009) (n = 3) in TIP and 0.055 (0.018) (n = 3) in MID. SUV was 9.1 (3.0) (n = 4) in TIP and 10.2 (4.0) (n = 4) in MID. K_{PAT} (n = 3) and SUV (n = 4) were 0.013 (0.0003) min^{-1} and 2.4 (0.7), respectively, in REF. In general, the changes in blood flow and metabolism overlapped, but in some patients a few high flow regions had low levels of fluoride uptakes close to that of intact bone. When we compared MID to the ungrafted side, and increase of more than 400% was found in overall bone metabolism, but only an increase of 60% in blood flow.

4 months after surgery (patients 1–3), the indices of bone metabolism declined by one third in most of the grafted regions studied when compared to the first study. In all patients, TIP metabolism was higher than MID. All 3 patients had higher values of SUV in the more proximal regions, ranging from 5.0 to 17 and all had at least one region with SUVs of 15 or more. Blood flow increased in patient 1 from low values in the first analysis, to about the same level as patients 2–3. Flows (mL/min/100 mL) were still up to 20 proximally and down to 5–8 more distally, approaching the levels seen contralaterally in REF, 4.6 (0.6) mL/min/100 mL.

1 year after surgery (patients 1–5), bone metabolism had declined further by 20–30% in the TIP area, but was stable in MID. As compared to the initial study, mean SUVs had fallen by 76% in TIP, but were still 130% higher than REF (p = 0.05). When we compared MID at 1 year with the value at 8 days, we found a reduction in SUVs of 86% (p = 0.02). The SUV of MID at 1 year was also 130% higher than that of REF at the initial study (p = 0.05). KPAT (min^{-1}) of TIP and MID were 0.024 (0.004) and 0.023 (0.006), respectively. In the proximal areas of the graft bed, we noted similar reduction in SUV and KPAT by 20–30%, as compared to the analysis at 4 months, but only 20–50% compared to the analysis at 8 days. K_{PAT} and SUV of REF were 0.0087 (0.0011) and 2.2 (1.1), respectively. Blood flow in most regions studied declined further, as compared to the first study, by 50% and to the second study, by 37%. However, the mean blood flow was still 30% higher than the REF. Small zones with persistently higher blood flow were seen in several patients in the trochanteric region. We measured the blood volumes in patients 4–5: and found an average of 3.3 mL/100 mL in both cases in REF. The average blood volumes in bone of the TIP and MID regions were 2.24 and 2.75 mL/100 mL in patients 4 and 5, respectively. Patient 4 had relatively large variations in the blood volume of grafted bone, but we found no correlation between this finding and the levels of fluoride uptake or blood flow. In patient 5, the distribution of graft blood volume tended to be more uniform.

Results of radial profÕes analysis (PPP)

We calculated the peak-to-peak distances in profiles (PPP) of ^{18}F-fluoride activity in the MID region in patients 1–5 and averaged 4 radial pro-

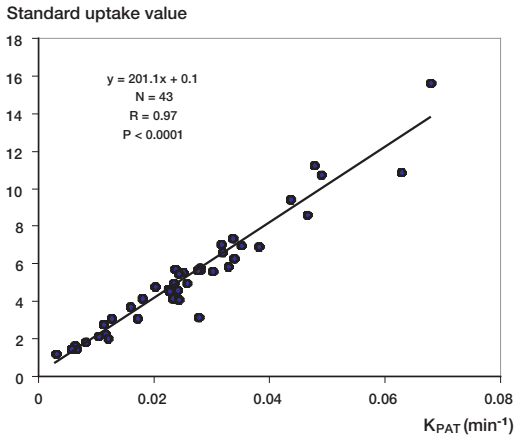

Figure 4. Plot of two quantitative measurements of the rate of bone metabolism. K_{PAT} is calculated by a kinetic model, using arterial blood sampling. SUV is determined by normalizing the regional uptake at one time according to the patient's weight and the amount of activity injected. We compared 43 distinct anatomical regions from 11 studies.

files through the center of the prosthesis stem of equal angles.

The average PPP at 1–8 days after surgery was 20.9 (0.9) mm and that at 1 year had declined to 15.8 (1.3) mm ($p = 0.05$). The inner profile slopes were steeper at the 1-year follow-up than on the initial study in all cases on visual inspection. Because the combined diameter of the stem and the surrounding cement layer was known, the findings from the PPP analysis confirmed at 1 year after surgery that bone was forming throughout the graft layer, with a maximum activity directly adjacent to the cement layer.

Comparison of kinetic and static derivatives of bone metabolism

In this study, using simple regression we found a linear and highly significant correlation between K_{PAT} and SUV (SUV = 201 (8.3) * K_{PAT} + 0.07 (0.25), $n = 43$, $r = 0.97$, $p < 0.001$). Values from 43 regions sampled from 11 studies were compared (Figure 4).

Discussion

Main findings

We aimed to use the PET technique to study blood flow and new bone formation in allografts surrounding the femoral component in revision THA with the impacted morselized bone allograft technique. The highest bone blood flow and fluoride uptakes occurred surprisingly early (8 days). The activity with time gradually declined in all Gruen zones, somewhat slower proximally. By applying the new concept of Radial Profile Analysis, we found that the diameter of the bone formation zone on transverse scans of the diaphysis declined from 21 mm at 1 week to 16 mm at 1 year, indicating a gradual in- and on-growth of new bone.

Tracers used in this study

We used [^{18}F]-fluoride PET to establish an index of regional bone metabolism, K_{PAT} (Hawkins et al. 1992, Piert et al. 1998). K_{PAT} defines the rate at which ^{18}F-ions are extracted from plasma and irreversibly deposited in bone mineral. This is an active and complex process of fluoride uptake (Schiepers et al. 1997). In a recent study (Piert et al. 2001) kinetic ^{18}F-fluoride PET was compared to the bone formation rate in pigs, as assessed by invasive bone histomorphometry, and a significant correlation was found.

We also made a semi-quantitative estimate of regional fluoride uptake, in the PET nomenclature called Standard Uptake Value, SUV. This type of measurement, usually used in clinical PET applications, because it can be calculated from a single tomographic image, does not require blood sampling. We tested SUV against K_{PAT} to assess the accuracy of SUV as a quantitative index of the bone metabolic rate.

We used [^{15}O] water PET to measure absolute values of regional bone blood flow in units mL/min/100 mL, a standard PET method in the study of blood flow in soft tissues, which has been used in bone as well (Raichle et al. 1983, Ashcroft et al. 1992, Ruotsalainen et al. 1997). Although theoretically feasible as a tracer of perfusion in all tissues, some assumptions about constants used in the [^{15}O] water model program were made in this study without experimental validation. However, as these assumptions affect absolute values in a linear fashion, comparisons of bone blood flow can still be done inter- and intra-individually.

We used [^{15}O] carbon monoxide PET to measure regional bone blood volumes in units of mL/100 mL (Iida et al. 1999). There should be no dispute

about the use of this technique. The main source of error is due to statistical noise in regions of low activity and sufficiently large sample regions should be used.

The reliability of our results, especially as regards the uptake of fluoride as early as at 8 days after surgery, must be determined. The uptake curve during the 50 min of the study is not that of passive diffusion, but that of an active uptake. The method may be criticized because the initially high fluoride uptake can reflect diffusion and fixation on naked bone particles. One of the patients was studied on the first day after surgery. At this time, the levels of both fluoride uptake and blood flow were similar to those of the healthy contralateral femur. It seems very likely that more naked bone particles should be available to fluoride ions in the interstitial fluid one day after surgery than at the follow-up after 8 days.

We found signs of intense osteoblastic activity in the graft area even 8 days after surgery, which were regarded as a regional increase in both fluoride uptake and blood flow. This biological phenomenon is probably facilitated by the graft material, as suggested by the finding of a less dramatic response in cortical femur adjacent to the inert plastic plug distal to the stem. The rapid occurrence of fluoride uptake should not be interpreted the formation of bone in the graft bed, but probably as a sign of intense osteoblastic activity in an early stage of bone healing adjacent to the graft layer.

Blood flow was increased adjacent to the graft bed after 8 days, suggesting that neovascularization is, indeed, swift. However, in the course of bone formation in the graft, we saw signs of uncoupling of the relation between bone blood flow and metabolic activity. Recent studies have suggested that this relation exists in normal bone, especially in bone marrow (Piert et al. 2001). This may not be true in a situation like our study, where bone marrow is scarce.

The blood volume in cortical bone and in graft material would of course be expected to be low shortly after surgery, which was also seen in our study. However, the combination of a subnormal blood volume and an increase in blood flow indicates that the regional capillary perfusion pressure rises shortly after surgery. This change in the vascular compartment is presumably due to a locally-derived stimulus from the activated bone cells or some factor directly derived from the graft material. It seems likely that an intense and prolonged challenge to the capillary flow reserve should act as a potent stimulus for neovascularization.

Both the histological data and the novel method of profile analysis used in our study suggest that the activity, reflected by the high fluoride uptake and an increase in blood flow shortly after surgery, was located at the interface between cortical bone and the graft. This is not surprising and similar findings have been reported in other studies of graft healing (Schliephake et al. 1999). 1 year later, it occurred more centrally, in close proximity to the cement layer surrounding the femoral prosthetic stem. The anatomical location and the apparent progression of the ^{18}F-uptake in a centripetal direction suggest that morselized, unprocessed, but fat-reduced bone allograft has an osteogenic effect. The signs of bone healing seen on the plain radiographs were supported by the swiftness of the healing process that we noted using PET. We have found one previous publication that analyzed the healing of a morselized bone allograft with PET (Piert et al. 1999). The bonegraft that was not reduced by fat had become "slightly condensed" in an acetabular defect, which probably means that it was less tightly impacted than in our study. Their method of studying bone healing was similar to ours. The rise in fluoride uptake was 200% after a mean of 1 month and 50% after mean 2.5 years.

PET findings in relatŠn to prevŠus histological studies

Our findings are supported by histological observations in 19 cases evaluated from 1 to 48 months after the same kind of surgery, using the same types of impaction instruments (Ullmark and Obrant 2002). In that study, the regeneration with both in-growth of fibrous tissue and new bone formation had started after 3–4 weeks. In all cases, healing was continuous during the first postoperative year. In one whole autopsied femur, analyzed after 4 years, healing was almost complete to living bone, except in the proximal part where some fibrous tissue was found. Another autopsied femur, examined 6 months after surgery (Ullmark and Linder 1998), also showed gradual bone regeneration in all regions. Even in this case healing was

somewhat slower in the most proximal part. The PET data accorded with these findings.

ImplicatŠns of study

To increase the healing capacity, we used fresh frozen unprocessed femoral head allografts. They were prepared with a method that reduces the amount of donor marrow fat, and thus favors the presence of fibrin clots mediating bone morphogenetic proteins. This was achieved by reducing fat in the chips and the design of the impaction phantoms containing small holes. This enables blood to enter the graft bed in its impacted state, and further defatting, which reduces the immunogenic properties of the graft (Thorén 1994). We used the matte femoral stem (Ra 1.5 μm) with a collar and of medium length (170 mm), a design that has a low tendency for subsidence.

No comparison has been made of the use of SUV and KPAT in the quantitative assessment of ^{18}F-uptake as corresponding to bone metabolism. Our data suggest that SUVs obtained relatively early after injection can be used instead of KPAT under the circumstances of our study. This could be helpful in future studies of bone formation after hip revision, because it allows a larger area of the patient to be scanned in one sequence. It also reduces the invasiveness of the procedure and widens the use of PET to more centers where blood sampling facilities are not available. The noninvasive determination of the dynamics of ^{18}F-uptake as corresponding to osteoblastic ingrowth in a femoral graft bed by the use of radial profiles analysis and serial PET seems feasible. This technique can be used with static images and should be easily automated, thereby increasing objectivity.

Study limitatŠns

Only a few patients were included in this study on the use of PET. Our approach was experimental to some extent and all tracers were not used on all occasions. However, the findings with PET resembled those obtained on histological examinations in previous studies and with the clinical and radiographic results in the same patients. Another limitation concerns the use of the [^{15}O] water model for measuring regional bone blood flow in absolute terms. Although the validity of our measurements supported by the relatively narrow range of values obtained from healthy femurs, technical questions like the distribution volume of water in various types of bone tissue remain to be settled before our data can be used for reference in future studies.

ConclusŠn

There is still much to be learned about the physiological processes taking place in a graft bed. The findings with PET of early regeneration of blood flow and ^{18}F-uptake, interpreted as osteoblastic activation in morselized allogenic bone grafts, agree with previous morphologic findings from biopsies in patients operated on with this method at revision THA. Thus, PET provides a relatively noninvasive method for studying metabolic events in bone and bone grafts in vivo. The information gained from such studies can be useful in the further refinement of surgical techniques such as the impacted morselized bone-grafting method.

Ashcroft G P, Evans N T S, Roeda D, Dodd M, Mallard J R, Porter R W, Smith F W. Measurement of blood flow in tibial fracture patients using positron emission tomography. J Bone Joint Surg (Br) 1992; 74: 673-7.

Blake G M, Park-Holohan S J, Cook G J, Fogelman I. Quantitative studies of bone with the use of ^{18}F-fluoride and 99mTc-methylene diphosphonate. Semin Nucl Med 2001; 31 (1): 28-49.

Charnley J. Numerical grading of clinical results. In: Low friction arthroplasty of the hip: theory and practice (Ed. Charnley J) Springer-Verlag 1979: 20-4.

Eldridge J D J, Smith E J, Hubble M J, Whitehouse S L, Learmonth I D. Massive early subsidence following femoral impaction grafting. J Arthroplasty 1997; 12 (5): 535-40.

Engelbrecht E, Heinert K. Klassifikation und Behandlungsrichtlinien von Knochensubstanzverlusten bei Revisionsoperationen am Huftgelenk-mittelfristige Ergebnisse. Primare und Revisionsalloarthroplastik Hrsg-Endo-Klinik, Hamburg, Berlin, etc: Springer-Verlag 1987: 189-201.

Gjedde A. High- and low- affinity transport of D-glucose from blood to brain. J Neurochem 1981; 36 (4): 1463-71.

Gjedde A. Calculation of cerebral glucose phosphorylation from brain uptake of glucose analogs in vivo: a re-examination. Brain Res Rev 1982; 4: 237-74.

Gruen T A, McNeice G M, Amstutz H C. "Modes of failure" of cemented stem-type femoral components. A radiographic analysis of loosening. Clin Orthop 1979; 141: 17-27.

Hawkins R A, Choi Y, Huang S C, Hoh C K, Dahlbom M, Schiepers C, Satyamurthy N, Barrio J R, Phelps M E. Evaluation of the skeletal kinetics of fluorine-18-fluoride ion with PET. J Nucl Med 1992; 33: 633-42.

Iida S, Harada Y, Ikenoue S, Moriya H. Measurement of bone marrow blood volume in the knee by positron emission tomography. Eur J Nucl Med 1999; 26 (6): 615-24.

Kärrholm J, Hultmark P, Carlsson L, Malchau H. Subsidence of a non-polished stem in revisions of the hip using impaction allograft. J Bone Joint Surg (Br) 1999; 81: 135-42.

Linder L. Cancellous impaction grafting in human femur: Histological and radiographic observations in 6 autopsy femurs and 8 biopsies. Acta Orthop Scand 2000; 71 (6): 543-52.

Mikhail W E M, Wretenberg P F, Weidenhielm L R A, Mikhail M N. Complex cemented revision using polished stem and morselized allograft. Arch Orthop Trauma Surg 1999; 119: 288-329.

Nelissen B G H H, Bauer T W, Weidenhielm L R A, Le Golvan D P, Mikhail W E M. Revision hip arthroplasty with the use of cement and impaction grafting, histological analysis of four cases. J Bone Joint Surg 1995 (Am); 77: 412-22.

Nivbrant B, Kärrholm J, Söderlund P. Cemented and cementless anteverted stems in revision surgery using impacted allograft. Thesis, University of Umeå, Sweden 1999.

Patlak C S, Blasberg R G, Fenstermacher J D. Graphical evaluation of blood-to-brain transfer constants from multiple-time uptake data. J Cereb Blood Flow Metab 1983; 3: 1-7.

Piert M, Zittel T T, Machulla H J, Becken G A, Jahn M, Maier G, Bares R, Becker H D. Blood flow measurements with [15O] H2O and [^{18}F] fluoride ion PET in porcine vertebrae. J Bone Mineral Research 1998; 13 (8): 1328-36.

Piert M, Winter E, Becker G A, Bilger K, Machulla H-J, Myller-Schauenburg W, Bares R, Becker H D. Allogenic bone graft viability after hip revision arthroplasty assessed by dynamic [^{18}F] fluoride ion positron emission tomography. Eur J Nucl Med 1999; 26 (6): 615-24.

Piert M, Zittel T, Becker G, Jahn M, Stahlschmidt A, Maier G, Machulla H J, Bares R. Assessment of porcine bone metabolism by dynamic [^{18}F] fluoride ion PET: Correlation with bone histomorphometry. J Nucl Med. 2001; 42 (7): 1091-100.

Raichle M E, Martin W R, Herscovitch P, Mintun M A, Markham J. Brain blood flow measured with intravenous H2(15)O. II. Implementation and validation. J Nucl Med 1983; 24 (9): 790-8.

Ruotsalainen U, Raitakari M, Nuutila P, Oikonen V, Sipilä H, Teräs M, Knuuti J, Bloomfield P M, Iida H. Quantitative blood flow measurement of skeletal muscle using oxygen-15-water and PET. J Nucl Med 1997; 38 (2): 314-9.

Schiepers Ch, Nuyts J, Bormans G, Dequerker J, Bouillon R, Mortelmans L, Verbruggen A, De Roo M. Fluoride kinetics of the axial skeleton measured in vivo with fluorine-18-fluoride PET. J Nucl Med 1997; 38 (2): 314-9.

Schliephake H, Berding G, Knapp W H, Sewilam S. Monitoring of graft perfusion and osteoblast activity in revascularised fibula segments using [^{18}F]-positron emission tomography. J Orthop Sci 1999; 4 (3): 216-22.

Thorén K. Lipid-extracted bone graft. Thesis, University of Lund, Sweden 1994.

Ullmark G. Bigger size and defatting of bone chips will increase cup stability. Arch Orthop Trauma Surg 2000; 120 (7/8): 445-7.

Ullmark G, Linder L. Histology of the femur after cancellous impaction grafting using a Charnley prosthesis. A case report. Arch Orthop Trauma Surg 1998; 117 (3): 170-2.

Ullmark G, Obrant K. Histology of impacted bone graft incorporation. J Arthroplasty 2002; 17 (2): 140-9.

Ullmark G, Hallin G, Nilsson O. Impacted corticocancellous allografts and cement for femoral revision of total hip arthroplasty using Lubinus and Charnley prostheses. J Arthroplasty 2002; 17 (2): 150-7.

van Biezen F C, ten Have B L E F, Verhaar J A N. Impaction bone-grafting of severely defective femora in revision total hip surgery. Acta Orthop Scand 2000; 71 (2): 135-42.